# Evaluation of the ITER cable in conduit conductor heat transfer

Nicollet S., Ciazynski, D., Duchateau J.L., Lacroix, B., Renard, B.

Association EURATOM-CEA, CEA/DSM/DRFC, CEA-Cadarache, F-13108 Saint Paul-lez-Durance, France

Convective heat transfer correlations in dual channel Cable In Conduit Conductor (CICC) are presented as functions of friction factor, and based on the Reynolds-Colburn analogy using the Stanton number. The developed thermohydraulic model determines helium temperatures in both channels, with the real geometrical spiral perforation. It is applied with pertinence to the Poloidal Field Full Size Joint Sample (PF-FSJS) and shows good agreement between the experimental measurements and the calculated temperatures, characterised by a 0.43 m space constant. The heat load applied in the bundle region induces density imbalance; the gravity effect in this vertical sample is evaluated and discussed.

## INTRODUCTION

The ITER Cable In Conduit Conductors, cooled by forced flow supercritical helium, are characterised by a dual channel : the bundle region where the superconducting strands are located and the central hole region delimited by the central spiral. During normal operation of the coils or transient safety discharge, heat loads are induced in the strands (AC losses) or transferred from the stainless steel case and plates (nuclear heating, radiation and eddy currents) to the conductor. An overheating of the bundle region can decrease the temperature margin, and the heat transfer from bundle to central hole is then a key factor.

## HEAT TRANSFER COEFFICIENT BETWEEN BUNDLE AND CENTRAL HOLE REGIONS

The main purpose is to determine the convective heat transfer between the bundle and central hole regions. Since little experimental data are available, the idea is to use the Reynolds-Colburn analogy (1) between fluid friction and heat transfer [1], associated with the friction factor data base. Expressed with the Stanton number St (2), the friction factor $f_{EU}$ (3) and indirectly the Nusselt number Nu (4), this analogy is valid for fully developed turbulent flow in central hole region ($Re_h$ near $10^5$) as well as for laminar flow in bundle region ($Re_b < 5000$), where Re (5) is the Reynolds number. The well known Colburn equation (6) for the smooth tube is a particular case of these analogy. Combining equation (1), (3) and (4), leads to equation (7), expressing the convective heat exchange coefficient $h_{conv}$ (W/m²K) from the experimental bundle region friction factor $f_{EU,b}$ on one hand [2] the central spiral $f_{EU,h}$ on the other hand [3], [4]. Superimposed on forced-convection, natural-convection effect influences the laminar heat-transfer coefficient [1]: this point is further developed in the gravity effect section.

The global heat exchange coefficient between the two region $h_{perfor}$ (8) can then be expressed in function of the spiral perforation ratio (perfor) of the gap length over the twist pitch length, and the heat exchange coefficients $h_{open}$ (9) and $h_{close}$ (10) corresponding to the open and closed zone of the spiral respectively. In the latter, the conduction through the spiral is taken into account with the ratio of the stainless steel conductivity $\lambda_{SS}$ (W/mK) over the spiral thickness e (m).

$$St . \Pr^{2/3} = f_{EU} / 8 \tag{1}$$

$$St = Nu / \mathrm{Re} . \Pr \tag{2}$$

$$\Delta P_f = (f_{EU}.m^2.U.L)/(8.\rho.A^3) \tag{3}$$

$$Nu = h_{conv}.Dh/\lambda \tag{4}$$

$$Re = \rho \cdot v \cdot Dh/\mu = 4 \cdot m/\mu \cdot U \tag{5}$$

$$Nu = 0.023.Re^{0.8}.Pr^{1/3} \tag{6}$$

$$h_{conv} = (f_{EU}.\lambda.Re.Pr^{1/3})/(8.Dh) \tag{7}$$

$$h_{perfor} = h_{open}.perfor + h_{close}.(1 - perfor) \tag{8}$$

$$1/h_{open} = 1/h_{conv,b} + 1/h_{conv,h} \tag{9}$$

$$1/h_{close} = 1/h_{open} + e/\lambda_{SS} \tag{10}$$

Where : Pr (-): Prandtl number; $\Delta P$ (MPa): pressure drop; m (kg/s): mass flow, $\rho$ (kg/m$^3$): helium density; U (m): wetted perimeter; L (m): Length; A (m²): cross section; Dh (m): hydraulic diameter of the channel; $\lambda$ (W/mK): helium thermal conductivity; $\mu$ (Pa.s): helium dynamic viscosity.


# A STEADY STATE CHARACTERSITIC SPACE CONSTANT MODEL

Using a steady state model of heat transfer [5], and under a few simplifications (helium specific heat independent of the temperature), the energy balance (11) is expressed in both channels of the CICC: the bundle and central hole regions, with mass flows $m_b$ and $m_h$ and temperatures $T_b$ and $T_h$ respectively. That leads to the differential equation (12) and introducing the characteristic space constant $\Lambda$ (13), the temperature gradient $(T_b-T_h)$ and the bundle temperature are determined analytically. In the heated region $(0<x<L_h)$, equation (14) and (15) are valid, with the maximal temperature gradient at the end of the heated region (16). In the non-heated zone ($Q_x=0$ W/m for $L_h<x<L_h+L_{nh}$), the temperature gradient (17) and bundle region temperature (18) are also expressed.

$$m_b.cp.dT_b = \left(Q_x - hU_{perfor}.(T_b - T_h)\right).dx \quad \text{and} \quad m_h.cp.dT_h = hU_{perfor}.(T_b - T_h).dx \tag{11a and 11b}$$

$$d(T_b - T_h) = \left(\frac{Q_x}{m_b.cp} - \frac{hU_{perfor}.(T_b - T_h).(m_b + m_h)}{m_b.m_h.cp}\right).dx = (\beta - \gamma.(T_b - T_h)).dx \tag{12}$$

$$\Lambda = \frac{1}{\gamma} = \frac{\alpha.(1-\alpha).m_{tot}.cp}{hU_{perfor}} \tag{13}$$

$$(T_b - T_h) = (Q_x.\Lambda/m_b.cp).(1 - e^{\frac{-x}{\Lambda}}) \tag{14}$$

$$T_b = T_0 + \frac{Q_x.x}{m_{tot}.cp} + \frac{\Lambda.Q_x}{cp}.\frac{m_h}{m_b.m_{tot}}.(1 - e^{\frac{-x}{\Lambda}}) \tag{15}$$

$$\Delta T_{max} = (Q_x.\Lambda/m_b.cp).(1 - e^{\frac{-L_h}{\Lambda}}) \tag{16}$$

$$(T_b - T_h) = \Delta T_{max}.e^{-\frac{(x-L_h)}{\Lambda}} \tag{17}$$

$$T_b = T_0 + \frac{Q_x.L_h}{m_{tot}.cp} + \frac{\Lambda.Q_x}{cp}.\frac{m_h}{m_b.m_{tot}}.(1 - e^{\frac{-L_h}{\Lambda}}).e^{\frac{-(x-L_h)}{\Lambda}} \tag{18}$$

Where : x (m): abscissa along the conductor axis (x=0 at the beginning of the heated zone); $L_h$ and $L_{nh}$(m): length of the heated and non-heated zone, respectively; cp (J/kgK): helium specific heat at constant pressure; $T_0$ (K): inlet temperature (x=0); $Q_x$ (W/m): linear heat power deposition in the bundle region; $hU_{perfor}$ (W/mK): heat transfer coefficient per length at the perimeter $U_{perfor}$ (associated with diameter $Dh_h$-e) , $\Delta T_{max}$ (K): maximal temperature gradient at the end of the heated zone (x=$L_h$), $\alpha$ (-): ratio (equation (15) of [4]) of bundle mass flow $m_b$ to total mass flow rate $m_{tot}$ ($m_{tot}=m_h+m_b$).

## APPLICATION TO THE PF-FSJS

The PF-FSJS prototype using NbTi conductors [6] (with two legs: left (L) and right (R)) was tested at the Sultan Facility. On each leg, were installed one heater (length $L_h$=0.4 m) at the sample top feeder entrance (x=0 at the heated zone beginning) and four sensors : T2 (x=0.747 m), T3 (x=1.017 m), T4 (x=1.564 m) measuring the bundle region temperature and T5 (x=2.190 m) measuring the mixing temperature $T_{inf}$, at the end of the joint. Figure 1 presents the temperature measurements for the calibration tests with a power Q of 12 W ($Q_x$=30 W/m) and a mass flow rate $m_{tot}$ of 8 g/s in each leg (inlet pressure $P_{in}$=1.02 MPa and temperature $T_0$=4.5 K). The calculation performed with the Gandalf code (with the associated subroutine concerning friction factor, heat exchange coefficient, heat loads) are also presented. The characteristic space constant (13) $\Lambda$=0.437 m is calculated at the average temperature $T_{ave}=T_0+(Q/m_{tot}.cp_0)$=4.96 K ($cp_0$=3270 J/kgK), with a heat transfer coefficient per unit length $hU_{perfor}$=13.9 W/mK ($\alpha$=0.297). The bundle and central hole temperatures are deduced from analytical relation (14), (15), (17) and (18). The good agreement between experimental measurements and calculation confirms the pertinence of the heat transfer model developed with the characteristic space constant.
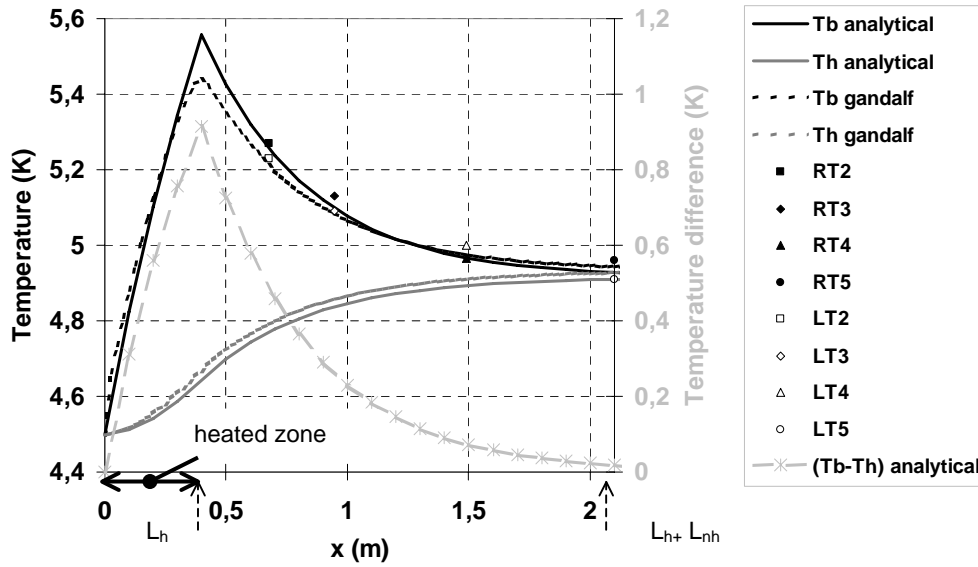


Figure 1 : PF-FSJS calculated and measured bundle and central hole temperatures ($Q_x$=30W/m, $m_{tot}$=8g/s)

## DISCUSSION AND EVALUATION OF GRAVITY EFFECT

When heating the PF-FSJS vertical sample with AC losses, some abnormal increases of the upstream temperature (T2) was observed. This was interpreted [7] as a signature of a blocked (zero) or reverse (thermosiphon) flow in the bundle region of the heated zone, which is schematised as in Figure 2. The pressure difference $\Delta P_{tot}$ equilibrium for both channels is expressed (19) over the corresponding hydraulic length (L=min ($L_h$,$\Lambda$)) as a function of the gravity g (9.81 m²/s) with $\theta$ angle between the CICC axis and horizontal direction; for the bundle region, $\Delta P_{f,b}$ (3) should be taken with a minus sign for direct (regular) flow pattern and a plus sign for reverse flow. The resolution of equation (19) is complex; a simple ratio r (20) can nevertheless be introduced to evaluate the importance of the gravity effect compared to the friction factor. A global bundle mass flow ratio $\alpha$ is determined as well to verify (19) with the assumption, that there is no mass flow redistribution over the hydraulic length. Table 1 sums up the experimental observations on the PF-FSJS (choke when overheating of T2) and the corresponding calculated values of $\alpha$ and r in function of Q and $m_{tot}$; the heat transfer coefficient $hU_{perfor}$ (near 10 W/mK at $m_{tot}$=4 g/s and 13 W/mK at $m_{tot}$=8 g/s) and the characteristic space constant $\Lambda$ (0.24 m at $m_{tot}$=4 g/s and 0.43 m at $m_{tot}$=8 g/s) are calculated with correlation (8) and (13) of first and second section respectively.

$$\Delta P_{tot} = P_{out} - P_{in} = \rho(T_h).g.x_{out}.\sin\theta - \Delta P_{f,h} = \rho(T_b).g.x_{out}.\sin\theta -/+ \Delta P_{f,b} \tag{19}$$

$$r = (\rho(T_h) - \rho(T_b)).g.\sin\theta.x_{out}/\Delta P_{f,h} \tag{20}$$
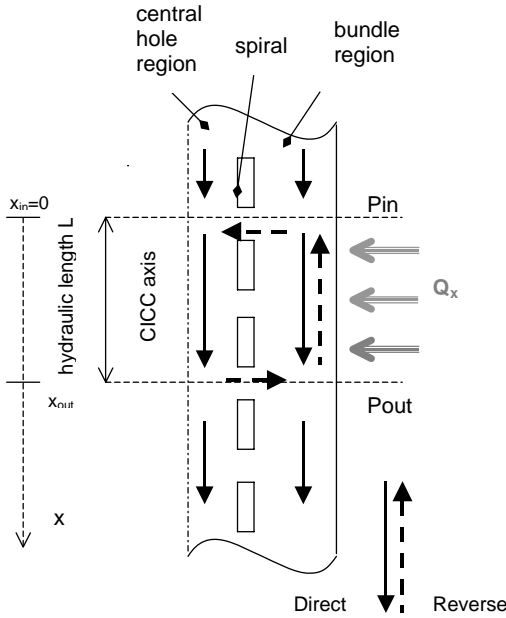
Figure 2 : Direct or reverse CICC flow pattern

Table 1 : Influence of gravity effect on the PF-FSJS

| experimental observation | | $m_{tot}=4g/s$ $10<hU_{perfor}<10.9$ W/mK $0.233<\Lambda<0.244$ m | $m_{tot}=8g/s$ $12.9<hU_{perfor}<14$ W/mK $0.421<\Lambda<0.437$ m |
|---|---|---|---|
| direct flow pattern | no choke | Q=0 W, $\alpha=0.239$, r=0 | Q=0 W, $\alpha=0.297$, r=0 |
| | no choke | Q=1 W, $\alpha=0.194$, r=0.32 | Q=6 W, $\alpha=0.254$, r=0.28 |
| | no choke | Q=2 W, $\alpha=0.106$, r=0.74 | Q=12 W, $\alpha=0.171$, r=0.65 |
| reverse | choke | Q=2.2 W, $\alpha=0.079$, r=0.83 | |

For the ITER Project and the vertical part of the Toroidal Field Coils, such a phenomenon should be estimated, especially during the 400 s power deposition (mainly nuclear heating) of plasma operation [8]. Considering the 18 coils with each 14 CICC turns on the Inner Leg Plasma Facing Wall first layer (with length near 8m), the maximal CICC power is $Q_x=2W/m$. With the interpolated correlation for the new spiral friction factor [9] ($Dh_h=9mm$, perfor=0.5 and $f_{EU,h}=0.45.Re_h^{-0.034}$), $m_{tot}=8$ g/s, Pin=5 MPa, and Tin=5 K, the bundle mass flow ratio, heat transfer coefficient and space constant are respectively $\alpha=0.656$, $hU_{perfor}=20.2$ W/mK and $\Lambda=0.41$ m. The resulting ratio r=0.023 allows to conclude that gravity effect is negligible compared to friction, and since $\alpha$ remains largely positive, no local overheating and reverse flow should occur in the bundle region.

CONCLUSION

New correlations for the convective heat exchange coefficient in CICC were applied with pertinence to express the global heat transfer. Depending on this last parameter and on the bundle mass flow ratio, a characteristic space constant was introduced in a steady state model, and analytical expressions of the bundle and central hole temperatures as well as the maximal temperature gradient were deduced. The gravity influence on the mass flow distribution was estimated and compared with experimental results for the PF-FSJS, especially in the case of a reverse-thermosiphon phenomenon at low mass flow. On the ITER TF Coils however, this phenomenon is expected to only slightly reduce the bundle mass flow.

REFERENCES

1. Holmann, J.P., Heat Transfer, ninth Edition, International Edition, Mc GrawHill, pp.230 and pp.272.
2. Nicollet S., Cloez H., Duchateau J.L., Serries J.P., Hydraulics of the ITER Toroidal Field Model Coil Cable-in-Conduit Condutors, in proceedings of the 20th Symposium on Fusion Technology, Marseille, France (1998) 771-774.
3. Nicollet S., Duchateau J.L., Fillunger H., Martinez A., Parodi S., Dual Channel Cable in Conduit Thermohydraulics : Influence of some Design Parameters, in IEEE Transactions on Applied Superconductivity (2000) 10 1102-1105.
4. Nicollet S., Duchateau, J.L., Fillunger, H., Martinez, A., Calculations of pressure drop and mass flow distribution in the toroidal field model coil of the ITER project, Cryogenics (2000) 40 569-575.
5. Park, S.H. Duchateau, J.L., The effect of Perforation between Hole and Bundle in CICC, Internal Note AIM/NTT-2003.035.
6. Decool, P., Design and manufacture of a prototype NbTi full-size joint sample for the ITER poloidal field coils, in proceedings of the 22nd Symposium on Fusion Technology, Helsinki, Finland (2002) 1165-1169
7. Ciazynski, D., Test of PF-FSJS in Sultan, Themohydraulics and Calibration, CRPP Workshop, Gstaad, January 2003.
8. Shatil, N., Thermo-hydraulic Analysis of TF Magnets, ITER FDR DDD, 11 Magnet, 2.1 CDA, Annex 10. Table 7 and 8
9. Nicollet, S., Cloez, H. Duchateau, J.L. Serries, J.P., Task CODES : Results of ITER type central spirals friction factor measurements in the OTHELLO facility and application to ITER Coils, Internal Note AIM/NTT-2003.018.